CHALMERS | GÖTEBORG UNIVERSITY

PREPRINT 2006:28

Rain-flow Fatigue Damage due to Nonlinear Combination of Vector Gaussian Loads

SAYAN GUPTA
IGOR RYCHLIK

Department of Mathematical Sciences
Division of Mathematical Statistics
CHALMERS UNIVERSITY OF TECHNOLOGY
GÖTEBORG UNIVERSITY
Göteborg Sweden 2006

Preprint 2006:28

Rain-flow Fatigue Damage due to Nonlinear Combination of Vector Gaussian Loads

Sayan Gupta and Igor Rychlik

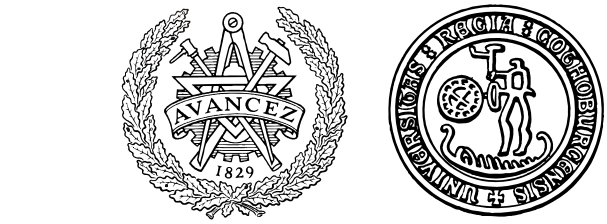

Department of Mathematical Sciences
Division of Mathematical Statistics
Chalmers University of Technology and Göteborg University
SE-412 96 Göteborg, Sweden
Göteborg, October 2006

Preprint 2006:28
ISSN 1652-9715

Matematiska vetenskaper
Göteborg 2006

Rain-flow Fatigue Damage due to Nonlinear Combination of Vector Gaussian Loads

Sayan Gupta *,1

Department of Civil Engineering, Section of Hydraulic Engineering, Technical University of Delft, Stevinweg 1, PO BOX 5048, 2600 GA, Delft, The Netherlands.

Igor Rychlik [2]

Center for Mathematical Sciences, University of Lund, Box 118, S-22100 Lund, Sweden

Abstract

The problem of estimating the mean rain-flow fatigue damage in randomly vibrating structures, is considered. The excitations are assumed to be through a vector of mutually correlated, stationary Gaussian loadings. The load effect leading to fatigue damage is considered to be a nonlinear function of the vector of excitation loads and is thus non-Gaussian. Its probabilistic characteristics are however unknown. The fatigue damage is assumed to follow a linear damage accumulation rule. Though exact expressions for the mean fatigue damage are difficult to determine, approximations and bounds for the mean rain-flow fatigue damage can be developed. Computing these quantities require estimating the mean level crossing statistics for the associated non-Gaussian response. For the special case when the load effect can be expressed as quadratic combinations of Gaussian processes, analytical expressions are developed for computing the level crossing statistics. These, in turn, are used to determine approximations and the bounds for the mean fatigue damage. The applicability of the proposed method is demonstrated through a numerical example. With respect to this example, a comparative study on the quality of the bounds and the approximations is carried out viz-a-viz the predictions from existing techniques available in the literature.

Key words: expected fatigue damage, rain-flow cycle counting, non-Gaussian, vector Gaussian process, nonlinear combination

1 Introduction

Estimating the mean fatigue damage in structures subjected to random loadings constitute a key step in predicting the remaining life time of the structure. In randomly vibrating large engineering structures, the load effect which causes fatigue damage, at a particular location in the structure, usually have contributions from a large number of components. Often, the resulting load effect is obtained as a nonlinear combination of these individual components and are thus non-Gaussian, even if the external loads are Gaussian. For example, if the stress tensor is not varying uniaxially, then nonlinear functions of the stress tensor are sometimes used to define the stress metric and then rain-flow counted to analyze the fatigue damage [25,26,34]. Another example is when weakly nonlinear systems have to be used to analyze responses to Gaussian loads. Here, the responses are often approximated by means of quadratic transfer functions (Volterra quadratic input-output model), which also leads to stresses which are non-Gaussian but as a function of a vector of Gaussian processes, viz.

$$Y(t) = g(X_1(t), \ldots, X_n(t)), \tag{1}$$

where, $g(\cdot)$ is a nonlinear deterministic function, $\{X_i(t)\}_{i=1}^n$ are stationary Gaussian processes and $Y(t)$ is the non-Gaussian process that causes fatigue damage.

Computing the fatigue damage from a random time history typically, involves (a) splitting the time history into a number of equivalent loading cycles corresponding to different amplitude levels, (b) estimating the associated incremental fatigue damage from Wöhler's curves, and (c) application of a suitable damage accumulation rule for computing the total fatigue damage. For a random load, the computed fatigue damage is a random variable. In predicting the remaining lifetime of a structure, the mean fatigue damage is the metric which is generally used. Computation of the mean fatigue damage can be carried out either in the time domain or in the frequency domain. The time domain approach involves repeated fatigue analysis on an ensemble of time histories having identical probabilistic characteristics. Subsequently, the mean fatigue damage is calculated as the first moment. The accuracy of the estimator is dependent on the sample size of the ensemble and is hence, time consuming and computationally intensive. On the other hand, frequency do-

* Corresponding author: S.Gupta@tudelft.nl, Phone: +31 15 27 88256, FAX:+31 15 27 85 124

Email addresses: S.Gupta@tudelft.nl (Sayan Gupta), igor@maths.lth.se (Igor Rychlik).

[1] Post-doctoral Researcher

[2] Professor

main approaches provide fast and elegant methods for estimating the mean fatigue damage. The latter approach is especially useful during the design process, when a large number of analyzes may need to be carried out. Here, the focus is on developing analytical expressions which relate the mean fatigue damage to the probabilistic characteristics, often in terms of the power spectral density function (PSD) and the probability density function (pdf) of the loading process. The present study belongs to this genre.

A key feature in fatigue estimation due to random loads lies in extracting and counting the equivalent load cycles from a random time history [35]. A number of cycle counting methods have been proposed in the literature, of which, the peak counting method, range counting method, level crossing method and the rain-flow cycle counting method are most widely used. Of these, the rain-flow cycle counting method [19] is regarded to lead to fatigue damage estimates which conform best with experimental observations. In this study, we limit our attention to developing approximations for the rain-flow fatigue damage.

The rain-flow cycle counting scheme, as proposed in [19], is highly nonlinear and difficult to model mathematically. To overcome this drawback, an equivalent but more suitable definition for mathematical derivations, has been suggested [28]. This has led to the development of approximations for the expected rain-flow fatigue damage due to stationary, Gaussian loads [30] and for loads having Markov properties [29,10]. An upper bound for the expected rain-flow damage was given in [31]. The bound coincides with the narrow-band approximation for Gaussian loads proposed already in [3]. For broad banded loads the method seriously overestimates the damage. Questions related to estimating the fatigue damage for broad-banded loadings and the accuracy when different counting methods are used, have been addressed in [4,24,36,40].

While most studies in the literature have focussed attention on Gaussian loads, many of the realistic applications of fatigue damage involve non-Gaussian loadings. However, studies on fatigue damage due to non-Gaussian loads are few and are of recent vintage. Semi-empirical expressions for predicting the rain-flow fatigue damage and its pdf have been developed in [2,37]. Here, the parameters of the models were determined from regression analyzes on an ensemble of non-Gaussian time histories. Analytical approximations for the mean fatigue damage for non-Gaussian loads obtained as monotonic transformations of stationary Gaussian loads have been developed in [38,39]. The present authors, in an earlier study [34], developed analytical expressions which approximate the rain-flow fatigue damage due to scalar non-Gaussian loads, obtained as non-monotonic transformations of stationary, Gaussian processes.

2 Problem Statement

We consider the problem of estimating the expected rain-flow fatigue damage caused by non-Gaussian load processes that can be expressed in the form as in Eq. (1). We assume that the fatigue damage due to $Y(t)$ can be expressed through the well known Palmgren-Miner's hypothesis [23,20]. Here, the accumulated linear fatigue damage caused by load $Y(t)$, $t \in [0, T]$, is denoted by D_T, and is given by $D_T = \sum \alpha S_j^b$, where, α and b are experimentally determined material properties, S denotes the stress levels for the counted cycles and the counter j indicates the number of equivalent stress cycles corresponding to an appropriate cycle counting scheme. Here, we only consider the rain-flow fatigue damage which we denote as D_T. Since $Y(t)$ is a random process, D_T is a random variable. The focus of this study is on developing approximations for $\mathsf{E}[D_T]$, where $\mathsf{E}[\cdot\,]$ is the expectation operator.

3 Expected Rain-flow Fatigue Damage

We turn now to computation of $\mathsf{E}[D_T]$, defined using rain-flow count and linear Palmer-Miner damage accumulation rule. For efficiency of presentation, we begin with a definition of the rain-flow fatigue damage.

3.1 Definition of Rain-flow Fatigue Damage

Assume that $x(t)$, $t \in [0, T]$ is a variable load function having a finite number of local maxima. Assume that a local maximum $v_i = x(t_i)$ in $x(t)$ is paired with one particular local minimum u_k, determined as follows:

- From the i-th local maximum (value v_i) one determines the lowest values in forward and backward directions between t_i and the nearest points at which $x(t)$ exceeds v_i.
- The larger (less negative) of those two values, denoted by u_i^{rfc}, is the rain-flow minimum paired with v_i, *i.e.*, u_i^{rfc} is the least drop before reaching the value v_i again on either side.
- Thus, the i^{th} rain-flow pair is (u_i^{rfc}, v_i), see Figure 1.

Note that for some local maxima v_i, the corresponding rain-flow minima u_i^{rfc} could lie outside the interval $[0, T]$. In such situations, the incomplete rain-flow cycle constitutes the so called residual and has to be handled separately. In this approach, we assume that the maximums in the residual, form cycles with the preceeding minimums in the residual.

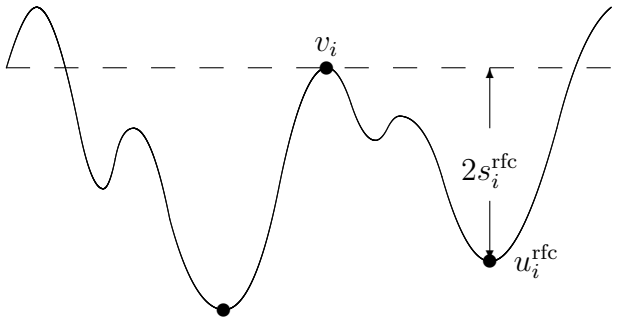

Fig. 1. Definition of rain-flow cycle.

The total damage D_T defined using the rain-flow method and applying the linear Palmgren-Miner damage accumulation rule leads to

$$D_T = \sum f(u_i^{\text{rfc}}, v_i) + D^{\text{res}}, \tag{2}$$

where D^{res} is the damage caused by cycles found in the residual.

An alternative definition for the rain-flow damage in Eq. (2) has been presented in [32]. Here, for a smooth load, $x(t)$, the rain-flow damage is given by

$$D_T = -\int_{-\infty}^{+\infty}\int_{-\infty}^{v} f_{12}(u,v)N(u,v)\,\mathrm{d}u\,\mathrm{d}v + \int_{-\infty}^{+\infty} f_2(v,v)N(u)\,\mathrm{d}u, \tag{3}$$

where, $f_2(u,v) = \frac{\partial f(u,v)}{\partial v}$ and $f_{12}(u,v) = \frac{\partial^2 f(u,v)}{\partial u \partial v}$. Here, for a smooth loading function $x(t)$,

- $N(u)$ is the number of up-crossings of level u by $x(t)$, $t \in [0,T]$, *i.e.*, the number of solutions to equation $x(t) = u$, such that, $\dot{x}(t) > 0$.
- $N(u,v)$ is the number of up-crossings of an interval $[u,v]$ by $x(t)$, *i.e.*, the number of solutions to equation system $x(t) = u, x(s) = v$, $0 \le t < s \le T$, such that, $\dot{x}(t) > 0, \dot{x}(s) > 0$ and for all z, $t < z < s$, $u < x(z) < v$. (Note that $N(u,u) = N(u)$).

Here, $\dot{x}(t)$ denotes derivative of $x(t)$ with respect to time t. Let (u_i, v_i) be a sequence of cycles found in the load $x(t)$ (both rain-flow cycles and the one found in the residual). It can then be shown that, $N(u,v)$ is equal to the number of pairs (u_i, v_i), such that $v_i > v$ and $u_i < u$ [32]. This is the basis for Eq. (3).

It must be noted that if $f(u,v) = (v-u)$, following Eq. (3), we get

$$D_T = \int_{-\infty}^{+\infty} N(u)\mathrm{d}u \tag{4}$$

as the first integral becomes equal to zero. If $f(u,v) = (v-u)^2$, Eq. (3) leads to $D_T = 2\int_{-\infty}^{+\infty}\int_{-\infty}^{v} N(u,v)\,\mathrm{d}u\,\mathrm{d}v$. Moreover, for $f(u,v) = (v-u)^\alpha$, where $\alpha \geq 2$, the second integral in Eq. (3) is always identically equal to zero.

In the following, for simplicity of presentation, we assume that the function $f(\cdot)$, defined in Eq.(2), to be such that $f_2(v,v) = 0$, for all v.

The rain-flow cycles measure the sizes of closed hysteresis loops, while the residual represents the memory of the material to previously experienced loads. The sizes and number of local extrema that constitute the residual will depend on the time when the structure was first loaded. Suppose that it happened at time $T_0 \leq 0$. Then the damage D_T, accumulated in the interval $[0,T]$, will also depend on T_0. More precisely, it will be given by Eq. (3) with $N(u,v)$ defined as follows: $N(u,v)$ is the number of solutions to equation system $x(t) = u, x(s) = v$, $0 \leq s \leq T$ and $T_0 \leq t < s$, such that, $\dot{x}(t) > 0, \dot{x}(s) > 0$ and for all z, $t < z < s$, $u < x(z) < v$. Clearly, the damage is a decreasing function of T_0.

3.2 Random Loads - Expected damage increase

For a random load $X(t)$, $0 \leq t \leq T$, the number of interval crossings, $N(u,v)$ is a random variable. Consequently, the rain-flow fatigue damage, at a particular time instant, is also a random variable. Determining the probabilistic characteristics of this variable is not easy. On the other hand, estimating the mean of the rain-flow fatigue damage is comparatively easier and is generally used to predict the expected life of the structure in question. As mentioned before, the damage depends on the time $T_0 \leq 0$ when the load started to act on the structure. Hence, in order to study the stationary damage increase in the period of length T, we assume that $T_0 = -\infty$.

If the joint pdf for cycle tops (v) and bottom (u) is known, then expected damage can be computed as

$$\mathsf{E}[D_T] = T\nu \int\int f(u,v) p^{\mathrm{rfc}}(u,v)\,\mathrm{d}u\,\mathrm{d}v, \tag{5}$$

where, $p^{\mathrm{rfc}}(u,v)$ is the joint pdf of u^{rfc} (minima) and v (maxima) of a rain-flow cycle. Note that the rain-flow matrix is the discretized pdf, $p^{\mathrm{rfc}}(u,v)$, which is then normalized so that elements in the matrix sums to one. The numerical value of expected damage, $\mathsf{E}[D_T]$, is obtained by

(a) multiplying (element-wise) matrix with cycles damages $f(\cdot)$ and the rain-flow matrix p^{rfc},
(b) subsequently, summing all the elements in the resultant matrix $f \cdot p^{\mathrm{rfc}}$, and
(c) finally, multiplying by the expected number of cycles $T\nu$.

Here, ν is the intensity of cycles, *i.e.*, the expected number of cycles in unit time.

Alternatively, using Eq. (3) and by changing order of integrations (Fubini's theorem) we have that

$$\mathsf{E}[D_T] = \int_{-\infty}^{+\infty} \int_{-\infty}^{v} f_{12}(u,v)\mathsf{E}[N(u,v)]\mathrm{d}u\,\mathrm{d}v. \tag{6}$$

Since for stationary processes, the expected number of intervals up-crossings are proportional to time duration T, the proportionality constant $\mu(u,v)$ can be termed as the intensity of interval up-crossings and is equal to $\mathsf{E}[N(u,v)]$ for $T=1$ and $T_0=-\infty$. The expected damage increase in period T can be shown to be proportional to the loading time duration T, and is written as

$$\mathsf{E}[D_T] = T\int_{-\infty}^{+\infty} \int_{-\infty}^{v} f_{12}(u,v)\mu(u,v)\,\mathrm{d}u\,\mathrm{d}v. \tag{7}$$

Consequently, we can write

$$d = \int_{-\infty}^{+\infty} \int_{-\infty}^{v} f_{12}(u,v)\mu(u,v)\,\mathrm{d}u\,\mathrm{d}v, \tag{8}$$

where, d can be called the damage intensity - the expected growth of the damage in unit time. The primary difficulty here is that, in general, there are only a few cases where the intensity $\mu(u,v)$ or the pdf $p^{\mathrm{rfc}}(u,v)$ can be computed exactly. The explicit results are available when loads possesses Markov property or have very simple structure.

3.3 Bound for the expected damage

In situations where explicit evaluation of $\mu(u,v)$ or $p^{\mathrm{rfc}}(u,v)$ is not possible, one can evaluate bounds for the intensity crossings. Thus, if $\mu(u)$ be the up-crossing intensity of level u by $X(t)$, *i.e.*, $\mathsf{E}[N(u)] = T\mu(u)$, then one can show that

$$\mu(u,v) \le \min[\mu(u,u),\mu(v,v)] = \hat{\mu}(u,v), \tag{9}$$

where, $\mu(u,u) = \mu(u)$. The proof is given in [31]. Note that $\mu(u,v) \le \mu(u)$ follows from the fact that for symmetrical loads the expected number of up-crossings of interval $[u,v]$ that end in $[0,T]$ is equal to the expected number of down-crossings of the interval $[u,v]$ that end in $[0,T]$. Since the intensity of down-crossings of level u is equal to $\mu(u)$, the bound follows. Consequently, one can write

$$\mathsf{E}[D_T] \le T\int_{-\infty}^{\infty} \int_{-\infty}^{v} f_{12}(u,v)\hat{\mu}(u,v)\,\mathrm{d}u\;\mathrm{d}v = T\cdot d^{+}. \tag{10}$$

The applicability of Eq. (10) lies in the ease of computation of the mean up-crossing rate, $\mu(u)$. This can be computed using Rice's formula [27], given by

$$\mu(u) = \int_0^\infty \dot{x} p_{X\dot{X}}(u, \dot{x}) \, \mathrm{d}\dot{x}, \tag{11}$$

where, $p_{X\dot{X}}(x, \dot{x})$ is the joint pdf of the process, $X(t)$, and its instantaneous time derivative, $\dot{X}(t)$. Clearly, $\mu(u)$ combined with Eq. (9) gives a conservative estimate of the expected damage.

3.3.1 The narrow band approximation

In the early 60s, the narrow band approximation was presented by Bendat [3] at a time when a definition for rain-flow cycle counting was not yet available. Bendat proposed that for a stress time history, $S(t)$, the cycle amplitude has the following probability distribution:

$$P(S \leq u) = 1 - \frac{\mu(u)}{\mu(0)}. \tag{12}$$

He also proposed to approximate the intensity of cycles by means of the zero crossing intensity, $\mu(0)$. It can be easily shown that the expected damage increase, estimated using Bendat's approach, coincides with the bound in Eq. (9) for the case of symmetric loads, such that, $\mu(-u) = \mu(u)$.

3.4 Asymptotic correction of the interval crossing intensity

The bounds for the expected damage, computed using the above arguments, may be extremely conservative when loads become broad-banded. In order to make the estimated damage less conservative, we focus on approximating $\hat{\mu}(u, v)$ using asymptotic properties of level crossings.

For large b, it is obvious that the contribution to the damage is mostly from the large cycles. Mathematically, this damage is given by the integral

$$-\int_{-\infty}^{u_0}\int_{v_0}^{+\infty} f_{12}(u, v)\mu(u, v) \, \mathrm{d}u \, \mathrm{d}v \leq -\int_{-\infty}^{u_0}\int_{v_0}^{+\infty} f_{12}(u, v) \min[\mu(u), \mu(v)] \mathrm{d}u \, \mathrm{d}v. \tag{13}$$

Now using the results derived in [15,16], one knows that asymptotically, *i.e.*, when u_0 tends to minus infinity while v_0 goes to plus infinity, the up-crossings of levels u and v, forms independent Poisson processes with intensities $\mu(u)$ and $\mu(v)$, respectively. Using this property, one can asymptotically approximate

$$\mu(u, v) \approx \frac{\mu(u)\mu(v)}{\mu(u) + \mu(v)}. \tag{14}$$

Hence

$$-\int_{-\infty}^{u_0}\int_{v_0}^{+\infty} f_{12}(u,v)\mu(u,v)\,\mathrm{d}u\,\mathrm{d}v \approx \int_{-\infty}^{u_0}\int_{v_0}^{+\infty} f_{12}(u,v)\frac{\mu(u)\mu(v)}{\mu(u)+\mu(v)}\,\mathrm{d}u\,\mathrm{d}v. \tag{15}$$

The formula (14) was first given in [13].

Let now $\tilde{\mu}(u,v) = \mu(u)\mu(v)/\{\mu(u)+\mu(v)\}$, for $u < u_0$ and $v > v_0$ and $\tilde{\mu}(u,v) = \hat{\mu}(u,v)$, otherwise. Then, one gets

$$d^{\text{poiss}} = \int_{-\infty}^{\infty}\int_{-\infty}^{v} f_{12}(u,v)\tilde{\mu}(u,v)\,\mathrm{d}u\ \mathrm{d}v, \tag{16}$$

where, d^{poiss} denotes the asymptotically corrected (approximate bound) for the damage intensity. Note that $d^{\text{poiss}} < d^{+}$.

3.5 The transformed Gaussian approximation

An alternative approach to approximating the interval crossing rate is to use the so called transformed Gaussian process. Here, one approximates the random (true) load $Y(t)$ by $\tilde{Y}(t) = G(X(t))$, where $G(\cdot)$ is a non-decreasing deterministic function and $X(t)$ is a stationary, Gaussian process. The expected damage intensity in $\tilde{Y}(t)$ can subsequently be estimated using the so called Markov chain of turning points. The method is well described in the literature, see e.g. [29,14,5,30,10,12,17]. The software to compute the approximation is available in WAFO, see [8]. In this approach, one needs to specify both the transformation $G(\cdot)$ and the spectral density $S(\omega)$ of $X(t)$.

The problem of selecting the transformation $G(\cdot)$ has been addressed in the literature. Usually, it is proposed to select $G(\cdot)$, such that the pdf of $Y(t)$ and $\tilde{Y}(t)$ coincide; see [38,39]. In [33], it was proposed to choose $G(\cdot)$, such that, the processes $Y(t)$ and $\tilde{Y}(t)$, have the same upcrossing intensity (up to a factor). A consequence of such transformations is that the bound coincides for both the loads, $Y(t)$ and $\tilde{Y}(t)$, and in the special case when $b = 1$, the corresponding expected rain-flow fatigue damages are identical. In the same paper, it was also discussed how to estimate both the transformation and the spectrum from the measured signal. For the quadratic type of responses studied in this paper, $X(t)$ can be assumed to be the linear (Gaussian) approximation of the response. The corresponding PSD, $S(\omega)$ can subsequently be easily determined. When the spectrum $S(\omega)$ and the transformation $G(\cdot)$ have been selected, the process $\tilde{Y}(t)$ is fully specified.

The use of transformed Gaussian processes is, however, not always recommended. For processes with large cycles that occur in clusters, e.g., due to potholes in roads [6] or when the load consists of a slowly varying process

with superimposed high frequency components, other methods need to be used; see [33]. However, for quadratic loads, the use of transformed Gaussian approach can be quite useful.

4 The second order responses

We now focus on deriving expressions for the response of randomly vibrating structures. The general form of the governing equations of motion, when discretized using finite elements, can be written as

$$\mathbf{M}\ddot{\mathbf{Y}}(t) + \mathbf{C}\dot{\mathbf{Y}}(t) + \mathbf{K}\mathbf{Y}(t) = \mathbf{F}(t). \tag{17}$$

Here, $\mathbf{M}$, $\mathbf{C}$ and $\mathbf{K}$ are the structure mass, damping and linear stiffness matrices of dimensions $n \times n$, $\ddot{\mathbf{Y}}(t)$, $\dot{\mathbf{Y}}(t)$ and $\mathbf{Y}(t)$ are respectively the vectors of nodal accelerations, velocities and displacements and $\mathbf{F}(t)$ is the vector for nodal forces, of size $n \times 1$. Let the focus of our attention be the structure response at a particular location of the structure and is denoted by $Y(t)$. We assume that the external excitations can be modeled as stationary Gaussian processes $\{X_j(t)\}_{j=1}^n$. This, in turn, means that the structure response can be expressed, at least in principle, as in Eq. (1).

Studying the increase in the expected rain-flow damage for quadratic responses is a very difficult problem. One obvious possible approach would be to simulate the loads and to compute the corresponding damage due to the response. However, in this approach, one needs to simulate an ensemble of long sequences of the response to get reliable estimates of the damage; see numerical example discussed later in this paper. This can be quite time consuming and expensive, especially at the design stage which includes repetitive iterations. Thus, there is a need to develop alternative methods which can lead to approximate estimates of the damage in a fast and reliable manner. In this paper, we give a general representation (see Eq. 38), for which most quadratic response problems can be written down. As has been already discussed, the crux of the problem lies in computing the mean crossing intensities for such processes. For computing the crossing intensity for loads which are represented in the form of Eq. 38, we consider two approaches- the first one is based on integration of Rice's formula (Eq. 11) using the Monte Carlo method [11], and the second, is the so called SORM asymptotic method, proposed first in [7]. Brief discussions on these methods are presented in the appendices of this paper. The computed crossing intensity, $\mu(u)$, is subsequently used to asses the expected damage as discussed in the previous section.

4.1 Definition of the g function in Eq. 1.

We now consider the special class of problems where the excitation load, $F(t)$, has a linear component, $F_L(t)$, and a quadratic component, $F_Q(t)$. Since Eq. (17) is linear, the response can be expressed as a sum $Y(t) = Y_L(t) + Y_Q(t)$, where, $Y_L(t)$ is the zero-mean Gaussian response when only $F_L(t)$ acts on the structure and $Y_Q(t)$ is the quadratic correction for nonlinearity due to the presence of load $F_Q(t)$.

Let us assume that $F_L(t)$ and $F_Q(t)$ are linear and quadratic functions of a zero-mean stationary, Gaussian random process, $\zeta(t)$, with a specified one sided PSD, $S_\zeta(\omega)$. We define the Gaussian load $\zeta(t)$, in the limit as N tends to infinity, to be of the form

$$\zeta_N(t) = \sum_{j=-N}^{N} \frac{\sigma_j}{2}(U_j - \mathrm{i}V_j)e^{\mathrm{i}\omega_j t}, \tag{18}$$

where, $U_j, V_j, j > 0$, are independent standard normal variables and $U_{-j} = U_j$, $V_{-j} = -V_j$, $\omega_{-j} = -\omega_j$. Moreover, $\omega_j = j\omega_c/N$ and $\sigma_j^2 = S_\zeta(\omega_j)\Delta\omega$, where, $j = 1, .., N$, $\sigma_0 = 0$, $\Delta\omega = \omega_c/N$, ω is the frequency defined in $0 \leq \omega \leq \omega_c$ and ω_c is the cut-off frequency, such that, $S_\zeta(\omega) = 0$, if $\omega > \omega_c$. For the sake of simplicity in representation, we write $\zeta(t)$ instead of $\zeta_N(t)$. Thus, in the discretized form, the linear response, $Y_L(t)$, is given by

$$Y_L(t) = \sum_{j=-N}^{N} \frac{\sigma_j}{2}H_1(\omega_j)(U_j - \mathrm{i}V_j)e^{\mathrm{i}\omega_j t}, \tag{19}$$

and the quadratic response, $Y_Q(t)$, is given by

$$Y_Q(t) = \sum_{j=-N}^{N}\sum_{k=-N}^{N} \frac{\sigma_j}{2}\frac{\sigma_k}{2}H_2(\omega_j, -\omega_k)(U_j - \mathrm{i}V_j)(U_k + \mathrm{i}V_k)e^{\mathrm{i}(\omega_j - \omega_k)t}. \tag{20}$$

Here, $H_1(\omega)$ and $H_2(\omega_1, \omega_2)$ are the linear and the quadratic transfer functions for the structural response at the desired location.

We next define

$$\mathbf{\Theta} = [(U_1 - \mathrm{i}V_1)e^{\mathrm{i}\omega_1 t}...(U_N - \mathrm{i}V_N)e^{\mathrm{i}\omega_N t}]', \tag{21}$$

where, the superscript $(')$ denotes matrix transpose. Next, we introduce a column vector

$$\mathbf{Z}(t) = \begin{bmatrix} \Re(\mathbf{\Theta}(t)) \\ \Im(\mathbf{\Theta}(t)) \end{bmatrix}', \tag{22}$$

where, $\Re(\cdot)$ and $\Im(\cdot)$ denote the real and imaginary parts of the arguments. Then, the linear part of the response $Y(t)$ can be written as

$$Y_L(t) = \begin{bmatrix} \Re(\mathbf{q}) \\ \Im(\mathbf{q}) \end{bmatrix}' \mathbf{Z}(t), \tag{23}$$

where, $\mathbf{q}$ is the column vector containing $[\sigma_j H_1(\omega_j)]$.

We next rewrite the quadratic response using the $\mathbf{Z}(t)$ process. We define the following matrices,

$$\begin{aligned} \mathbf{Q} &= [q_{mn}], \quad q_{mn} = H_2(\omega_m, -\omega_n)\sigma_m\sigma_n, \\ \mathbf{R} &= [r_{mn}], \quad r_{mn} = H_2(\omega_m, \omega_n)\sigma_m\sigma_n, \\ \mathbf{W} &= [w_{mn}], \quad w_{mm} = -\omega_m, \text{ and } w_{mn} = 0 \text{ if } m \neq n, \end{aligned} \tag{24}$$

where, $m, n = 1, .., N$. Now introducing the matrix

$$\mathbf{A} = \begin{bmatrix} \Re(\mathbf{Q}) + \Re(\mathbf{R}) & \Im(\mathbf{Q}) - \Im(\mathbf{R}) \\ \Im(\mathbf{Q})' - \Im(\mathbf{R})' & \Re(\mathbf{Q}) - \Re(\mathbf{R}) \end{bmatrix}, \tag{25}$$

the quadratic response can be written as

$$Y_Q(t) = \frac{1}{2}\mathbf{Z}(t)'\mathbf{A}\mathbf{Z}(t). \tag{26}$$

Consequently, the response $Y(t)$ can now be expressed in terms of $2N$ independent, zero-mean, unit variance processes, $\{Z_i(t)\}_{i=1}^{2N}$, as follows:

$$Y(t) = \tilde{g}(\mathbf{Z}(t)) = \begin{bmatrix} \Re(\mathbf{q}) \\ \Im(\mathbf{q}) \end{bmatrix}' \mathbf{Z}(t) + \frac{1}{2}\mathbf{Z}(t)'\mathbf{A}\mathbf{Z}(t). \tag{27}$$

Here, $\mathrm{Cov}[\mathbf{Z}(0), \mathbf{Z}(0)] = \mathbf{I}$, where, $\mathbf{I}$ is the identity matrix of size $2N \times 2N$. The auto- and cross- covariance between $\mathbf{Z}(t)$ and its time derivative $\dot{\mathbf{Z}}(t)$ are given by

$$\mathrm{Cov}[\mathbf{Z}(0), \dot{\mathbf{Z}}(0)] = \begin{bmatrix} \mathbf{0} & -\mathbf{W} \\ \mathbf{W} & \mathbf{0}, \end{bmatrix} \tag{28}$$

$$\mathrm{Cov}[\dot{\mathbf{Z}}(0), \dot{\mathbf{Z}}(0)] = \begin{bmatrix} \mathbf{W}^2 & \mathbf{0} \\ \mathbf{0} & \mathbf{W}^2 \end{bmatrix}, \tag{29}$$

where, $\mathbf{0}$ is a $2N \times 2N$ matrix with all elements being zeros. Computation of the mean up-crossing rate of $Y(t)$ can be carried out using the algorithms presented in the appendices.

4.2 The standard representation of the quadratic responses

The limitation of using Eq. (27) is that for accurate representation, the number of discretized frequencies, N should be large, which, in turn, introduces a large number of random variables into the formulation. This, in turn, requires larger computational effort while calculating the mean up-crossing rate, $\mu_Y(u)$. We next focus on an approach which allows using large number of frequencies to be used but still keeps N relatively low.

Since the matrix $\mathbf{A}$ of size $2N \times 2N$ is real and symmetrical, it can be diagonalized. Let $\mathbf{P}$ be the matrix containing the ortho-normal eigenvectors of $\mathbf{A}$ and let $\mathbf{\Lambda}$ be the diagonal matrix with eigenvalues λ_j of $\mathbf{A}$ on the diagonal, such that,

$$\mathbf{A} = \mathbf{P}\mathbf{\Lambda}\mathbf{P}^{'}. \tag{30}$$

Sorting the eigenvectors in such a way, so that $|\lambda_1| \geq |\lambda_2| \geq ...|\lambda_{2N}|$, then $Y_Q(t)$ can be represented as

$$Y_Q(t) = \frac{1}{2}\{\mathbf{P}^{'}\mathbf{Z}(t)\}^{'}\mathbf{\Lambda}\{\mathbf{P}^{'}\mathbf{Z}(t)\} = \frac{1}{2}\sum_{j=1}^{2N}\lambda_j X_j^2(t), \tag{31}$$

where, $\mathbf{X}^{'}(t) = [X_1(t), .., X_{2N}(t)] = \mathbf{Z}(t)^{'}\mathbf{P}$ are zero-mean, stationary Gaussian processes. In addition, since $\mathbf{Z}(t) = \mathbf{P}\mathbf{X}(t)$, $Y_L(t)$ can be expressed as

$$Y_L(t) = \begin{bmatrix} \Re(\mathbf{q}) \\ \Im(\mathbf{q}) \end{bmatrix}^{'} \mathbf{P}\mathbf{X}(t) = [\gamma_1, .., \gamma_{2N}]\mathbf{X}(t). \tag{32}$$

Now the response $Y(t)$ can be written as

$$Y(t) = \tilde{g}(\mathbf{P}\mathbf{X}(t)) = g(\mathbf{X}(t)) = \sum_{j=1}^{2N}\gamma_j X_j(t) + \frac{1}{2}\sum_{j=1}^{2N}\lambda_j X_j^2(t), \tag{33}$$

which is a function of $2N$ stationary Gaussian processes $\mathbf{X}(t)$. Clearly, the expression in Eq.(33) is simpler than in Eq. (27). The corresponding covariance matrices for $\mathbf{X}(t)$ and its time derivative are more complicated and are given by $\mathrm{Cov}[\mathbf{X}(0), \mathbf{X}(0)] = \mathbf{I}$ and

$$\mathrm{Cov}[\mathbf{X}(0), \dot{\mathbf{X}}(0)] = \mathbf{P}^T \begin{bmatrix} \mathbf{0} & -\mathbf{W} \\ \mathbf{W} & \mathbf{0} \end{bmatrix} \mathbf{P}, \tag{34}$$

$$\mathrm{Cov}[\dot{\mathbf{X}}(0), \dot{\mathbf{X}}(0)] = \mathbf{P}^T \begin{bmatrix} \mathbf{W}^2 & \mathbf{0} \\ \mathbf{0} & \mathbf{W}^2 \end{bmatrix} \mathbf{P}, \tag{35}$$

which are usually not diagonal matrices. However, the advantage of using Eq. (33) is that when the absolute values of coefficients $|\lambda_m|$, $m > k$ are close to zero, the associated terms can be omitted. This leads to the following truncated representation of $Y(t)$, given by

$$Y^{\text{app}}(t) = \sum_{j=1}^{k+1} \hat{\gamma}_j \hat{X}_j(t) + \frac{1}{2} \sum_{j=1}^{k+1} \hat{\lambda}_j \hat{X}_j^{\,2}(t), \tag{36}$$

where, $k \leq 2N$, $\hat{\lambda}_{k+1} = 0$, $\hat{\gamma}_{k+1} = \sqrt{\sum_{j=k+1}^{2N} \gamma_j^2}$ and $\hat{X}_j(t) = X_j(t)$ for $j \leq k$ and $\hat{X}_{k+1}(t) = \sum_{j=k+1}^{N} \gamma_j / \hat{\gamma}_{k+1} X_j(t)$. Thus, $\hat{X}_{k+1}(t)$ is a zero-mean Gaussian process with variance equal to $\sum_{j=k+1}^{2N} \gamma_j^2 / \hat{\gamma}_{k+1}^2$. The index k can be chosen using the following method. First, note that $\text{Var}[Y(t)] - \text{Var}[Y^{\text{app}}(t)] = 2 \sum_{j=k+1}^{2N} \lambda_j^2$. Next, k is chosen so that the variance of $Y^{\text{app}}(t)$ differs by less than $\epsilon\%$ from the exact, *i.e.*,

$$\text{Var}[Y(t)] - \text{Var}[Y^{\text{app}}(t)] \leq \frac{\epsilon}{100} \text{Var}[Y(t)]. \tag{37}$$

In this case also, we can use the algorithms discussed in the appendices, for computing the mean up-crossing rate $\mu_Y(u)$. However, certain modifications may be carried out which can lead to simplification in the application of the method. This requires rewriting the response $Y(t)$, as

$$Y(t) = \sum_{i=1}^{k} \{\Gamma_i X_i(t) + \Lambda_i X_i^2(t)\} + \Gamma_{k+1} X_{k+1}(t) = Y_{NG}(t) + Y_G(t). \tag{38}$$

Clearly the process $Y^{\text{app}}(t)$ is of form of Eq. (38). It is also obvious that $Y_{NG}(t)$ is a non-Gaussian process and $Y_G(t)$ is a Gaussian process. Appendix 2 details a different approach for computing the mean up-crossing rate, which simplifies the computations presented in Appendix 1.

Finally, it must be noted that a Gaussian approximation for $Y(t)$ can be obtained by letting all $\Lambda_i = 0$ in Eq. (38). This leads to the following Gaussian approximation $Y_L(t)$, given by

$$Y_L(t) = \sum_{i=1}^{k+1} \Gamma_i X_i(t). \tag{39}$$

In the remaining sections of this paper, the transformed Gaussian approximation for $Y(t)$ will be approximated by $G(Y_L(t))$.)

5 Numerical Example and Discussion

The theory proposed in this paper is illustrated through a numerical example. The example considers the rain-flow fatigue damage at the support of a cantilever beam, subjected to randomly varying wind loads. The wind loads are modeled as stationary Gaussian processes. The forces imparted on the beam are obtained as quadratic functions of the wind loads. Consequently, the theory proposed in this paper, have been used for assessing the mean fatigue damage. The predictions have been compared with those obtained from full scale Monte Carlo simulations. This involves digital generation of an ensemble of time histories for the response quantities of interest, from the available PSD functions. Corresponding to each sample time history, a deterministic analysis is carried out using the WAFO toolbox [8] to compute the associated rain-flow fatigue damage. The expected fatigue damage is subsequently computed as the first moment of the computed fatigue damages.

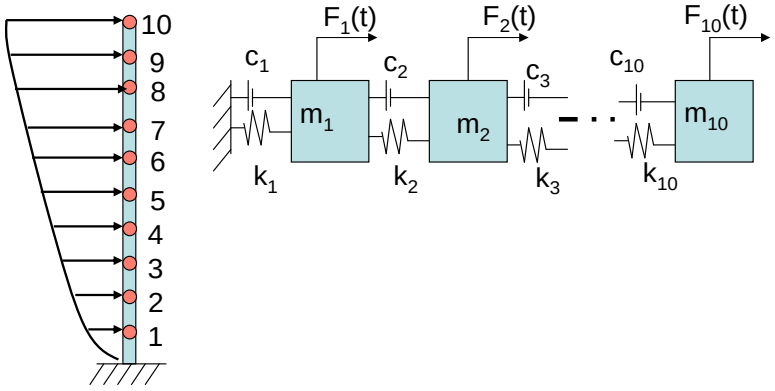

Fig. 2. Schematic diagram of the 10-dof cantilever beam subjected to random wind excitations.

The wind velocity is modeled as a stationary Gaussian process with specified mean wind speed, ζ_m, and PSD, $S_\zeta(\omega)$. The force due to wind loadings is given by $F(t) = 1/2 C_d \rho l b (\zeta(t) + \zeta_m)^2$, where, $\zeta(t)$ is a zero-mean Gaussian random process denoting the wind velocity at the tip of the beam, C_d is the drag coefficient, ρ is the air density and l and b are the dimensions of the structure. The beam is modeled as a simple lumped-mass model of 10-degrees-of-freedom. The variation of the wind velocity along the beam span is taken to be deterministic and is assumed to be parabolic, see Fig. 2. The normalized constants, $\{\chi_i\}_{i=1}^{10}$, are used to denote the wind velocity profile and are such that the maximum velocity is at the beam tip. The Davenport spectrum is assumed for $S_\zeta(\omega)$, and is given by

$$S_\zeta(\omega) = \kappa \frac{\zeta_f^2}{n} \frac{x^2}{(1+x^2)^{4/3}}, \tag{40}$$

where, $x = (L_{\text{ref}}/z)(\omega z/\zeta_{10}) = (1200/z)f$, $f = nz/\zeta_z$ is the normalized fre-

quency, $n = \omega/(2\pi)$ is the frequency in Hz, $S_\zeta(n)$ is the PSD of $\zeta(t)$ in $\mathrm{m^2 s^{-2} Hz^{-1}}$, z is the distance from the fixed end in m, ζ_z is the mean wind speed in m/s measured at distance z from the support, κ is the surface drag coefficient, ζ_f is the friction velocity in m/s and L_{ref} is the representative scale length. Denoting $\eta = 0.5 C_d \rho l b = 0.0250$, the wind force $F(t)$ can be expressed in terms of two dynamic components $F_l(t) = 2\eta\zeta_m\zeta(t)$ and $F_q(t) = \eta\zeta(t)^2$. The contribution from the mean wind velocity, $\eta\zeta_m^2$, acts as a constant load and has no bearing on the dynamic response of the structure.

The dynamic analysis is carried out by modeling the beam as a simple 10-degree-of-freedom lumped-mass model. The governing equations of motion are as in Eq. (17), with $\mathbf{F}(t) = \boldsymbol{\Upsilon}(F_l(t) + F_q(t))$. Here, $\boldsymbol{\Upsilon}$ is the influence matrix of size 10×1, whose elements denote the constants χ_i, $(i = 1, .., 10)$. The damping is assumed to be proportional, such that $\mathbf{C} = \eta_1\mathbf{M} + \eta_2\mathbf{K}$, where, η_1 and η_2 are the mass and stiffness proportionality constants. An eigenvalue analysis reveals that the first five natural frequencies of the structure are 2.32, 6.90, 11.32, 15.49 and 19.32 rad/s respectively. Assuming that damping is 10% in the first two modes, we get $\eta_1 = 0.3467$ and $\eta_2 = 0.0217$.

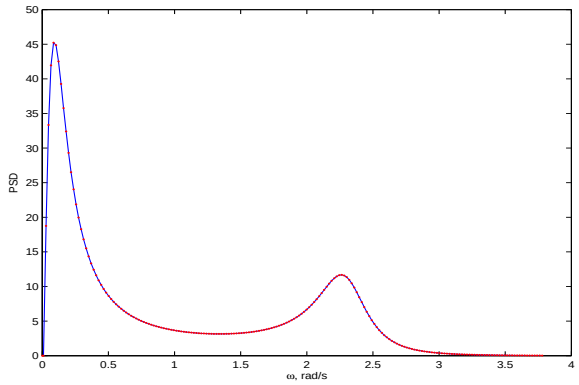

Fig. 3. Power spectral density function for $Y_L(t)$.

The maximum stresses are developed at the base of the cantilever beam and the rain-flow fatigue damage are calculated for this location. $\zeta(t)$ is modeled as a Gaussian process and is expressed using the approximation in Eq. (18). Since structure behavior is assumed to be linear (see Eq. 17), the response process can be expressed as a sum $Y(t) = Y_L(t) + Y_Q(t)$, where, $Y_L(t)$ is the Gaussian response when only $F_L(t)$ acts on the structure and $Y_Q(t)$ is the quadratic correction for nonlinearity due to the presence of load $F_Q(t)$. This enables rewriting the response $Y(t)$ as in Eq. (27) and as in Eq. (33). Here, the linear and quadratic transfer functions are obtained as

$$H_1(\omega) = [-\omega^2\mathbf{M} + \mathrm{i}\omega\mathbf{C} + \mathbf{K}]^{-1}\boldsymbol{\Upsilon} \tag{41}$$

$$H_2(\omega_1, \omega_2) = H_1(\omega_1 + \omega_2). \tag{42}$$

In this example, we discretized the PSD, $S_\zeta(\omega)$, into 200 segments, *i.e.*, $N =$

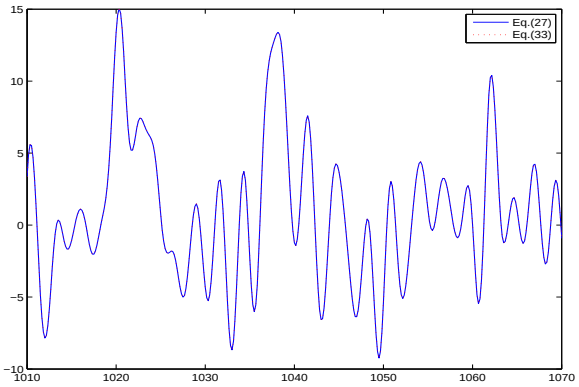

Fig. 4. Sample time history of response $Y(t)$.

200. Thus, the response $Y(t)$, is obtained as a nonlinear combination of a 400-dimensional vector of random processes $\mathbf{X}(t)$. Figure 3 illustrates the PSD of $Y_L(t)$. Figure 4 illustrates a sample time history of stress, $Y(t)$, developed at the root of the beam, calculated using Eq. (27) and Eq. (33). This illustrates that both these representations are equivalent.

5.1 Number of quadratic terms in Eq.(36) and accuracy of estimates of $\mu_Y(u)$

We next focus on fixing k in Eq. (36). Figure 5 illustrates the variation of k with respect to ϵ. We consider $\epsilon = 0.3$ and correspondingly, k turns out to be equal to 9. The response can now be approximated by $Y^{\text{app}}(t)$ as in Eq. (36), containing 10 terms. Figure 6 compares a sample response time history $Y^{\text{app}}(t)$ with $k = 9$ and with $Y(t)$ (when there are no truncations *i.e.*, $k = 400$). A very good agreement between the two representations is observed.

The accuracy of this representation in estimating $\mu_Y(u)$, can be verified from Fig. 7. Here, we present a comparison between the estimated upcrossing rates for $Y(t)$, when Monte Carlo simulations are used on an ensemble of 100 time

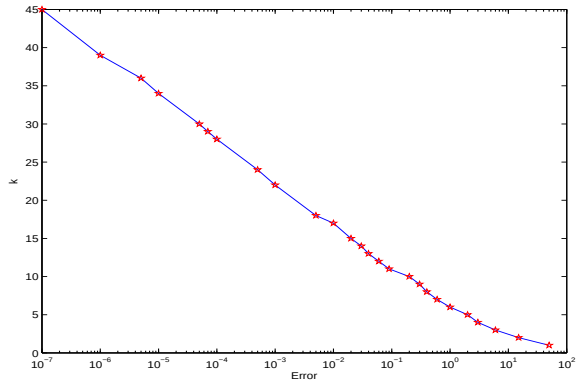

Fig. 5. Number of terms required in Eq.(36) for different values of percentage error, ϵ %.

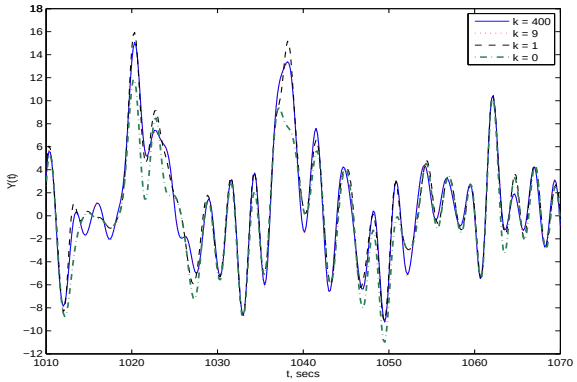

Fig. 6. Effect of truncation of terms in the representation of $Y(t)$.

histories consisting of $k = 400$ and when $k = 9$. The corresponding comparison of the predicted level crossing rates between the integration method (Appendix 1) and the SORM approach (Appendix 3) is shown in Fig. 8 in the log-scale.

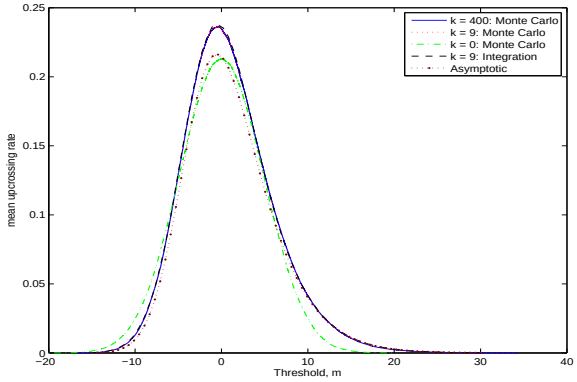

Fig. 7. Estimated up-crossing rates, $\mu_Y(u)$, using different methods, when $k = 9$ in Eq. (36).

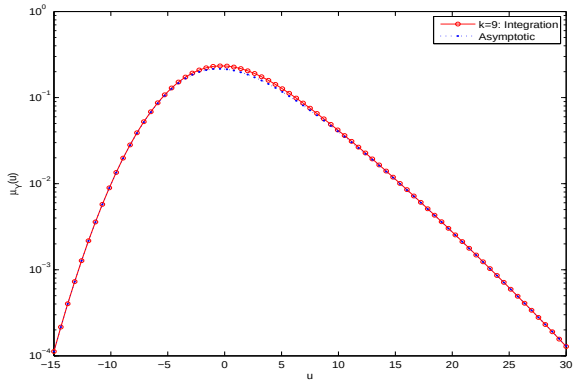

Fig. 8. Comparison of estimated $\mu_Y(u)$ between the Integration method and Asymptotic method.

We next explore the possibility of further truncation of quadratic terms in Eq. (36). We consider the case where $k = 1$. Here, there is only one quadratic term in Eq. (36) and corresponds to $\epsilon = 50$. For this example, the representation

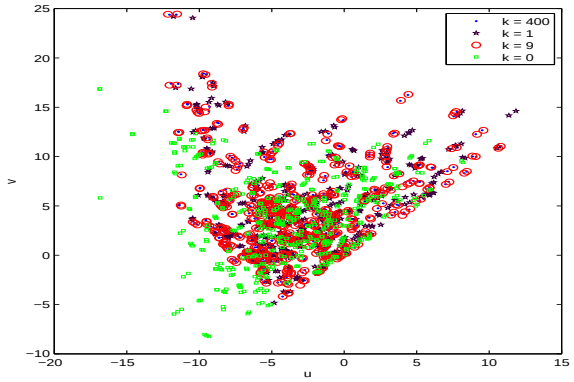

Fig. 9. Rain-flow cycles for sample $Y(t)$.

is still quite good; see Fig. 6. However, Fig. 9 reveals that there are differences in the identified rain-flow cycles. Table 1 presents a comparison of the expected rain-flow fatigue damages for the cases $k = 400$, $k = 9$ and $k = 1$ for various levels of $\alpha = 6.9 \times 10^{-(6+b)}$ and b. Figure 10 compares the predicted $\mu_Y(u)$ for the case when $k = 1$, as obtained by Monte Carlo simulations as well as when they are computed using the theory presented in Appendix 1. It can be observed that for negative threshold levels, the upcrossing rates are underestimated, when Eq. (36) contains only one quadratic term. However, the predicted upcrossing rates using Monte Carlo simulations and the theory presented in Appendix 1 are in good agreement (though erroneous), for all threshold levels. This indicates the robustness of the theory presented in Appendix 1. The differences with the benchmark can be attributed to the truncation of too many terms resulting in about 50% of the quadratic variability being lost.

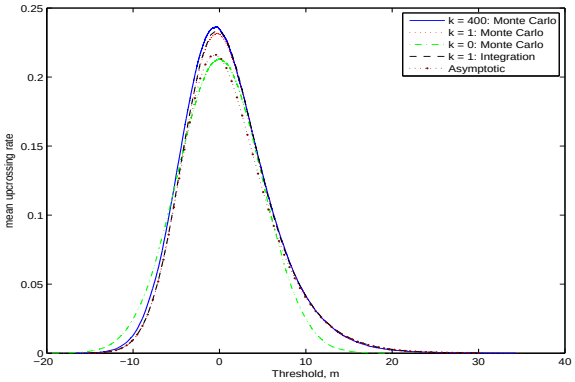

Fig. 10. Estimated up-crossing rates, $\mu_Y(u)$, using different methods, when $k = 1$.

We next explore the possibility of doing away with quadratic terms altogether by taking $k = 0$. Thus, Eq. (36), contains only linear terms and $Y(t) = Y_L(t)$, is a Gaussian random process. Figure 4 compares the corresponding sample time history with the case when $k = 400$. We observe that some cycles are missed and the amplitudes of the rain-flow cycles are underestimated (see also. Fig.

Table 1
Expected rain-flow fatigue damage, $f(u,v) = \alpha(v-u)^b$, $T = 1500$s, $\alpha = 6.9 \times 10^{-(6+b)}$; k in $\mathsf{E}[D^k]$, d_k^+ and d_k^{poiss} refers to numerical value of k in Eq.(36).

b	$\mathsf{E}[D_T^{400}]$	$\mathsf{E}[D_T^9]$	$\mathsf{E}[D_T^1]$	$\mathsf{E}[D_T^0]$	Td_9^+	Td_1^+	Td_9^{poiss}	Td_1^{poiss}
1	0.0029	0.0029	0.0028	0.0027	0.0029	0.0028	-	-
2	0.0038	0.0038	0.0036	0.0032	0.0047	0.0044	0.0047	0.0044
3	0.0065	0.0065	0.0061	0.0051	0.0093	0.0086	0.0091	0.0084
4	0.0140	0.0140	0.0131	0.0097	0.0219	0.0197	0.0206	0.0186
5	0.0354	0.0354	0.0333	0.0214	0.0588	0.0514	0.0534	0.0467
6	0.1014	0.1013	0.0958	0.0517	0.1777	0.1492	0.1557	0.1307

9). The estimated $\mu_Y(u)$ also significantly differ from the benchmark values-underestimated for most threshold values (see Fig. 7 and 10). The computed rain-flow fatigue damages, tabulated in Table 1, also clearly show that the predictions are significantly different if $k = 0$. This highlights the importance of taking into account the non-Gaussian features of the structure response.

It must be noted that by truncating from 400 to 9 quadratic terms, substantial reduction in computational effort is achieved without introducing any significant truncation error. On the other hand, further reduction to just one quadratic term does not provide any significant gain in terms of computational costs but introduces discretization errors. Clearly, the truncation to 9 quadratic and one Gaussian component perfectly describes the variability of the stresses at the location where the damage due to fatigue is of interest. One could ask the question whether there would be a difference if one wished to compute the one year value of the load, *i.e.*, the level u which has upcrossing intensity 3.2×10^{-8}. This is equivalent to one crossing of the level u in $T = 366 \times 24 \times 365$ s. Thus, the one year levels are computed to be 54.82, 54.80 and 54.78 for the cases when $k = 1$, $k = 9$ and $k = 20$ respectively. The result that asymptotically only one quadratic term is needed is not surprising. As has been discussed in Appendix 3, for quadratic loads the term with highest coefficient λ determines the asymptotic properties. It may be noted here, that for the case of extreme responses, the Monte Carlo integration of Rice's formula may not always be an appropriate method, especially if k is large. This is because the size of the vector of random variables that need to be simulated for the Monte Carlo integration may be prohibitively large. On the other hand, the asymptotic SORM method gives very accurate results at a much less computational cost. It can thus be concluded that the process $Y(t)$ with 9 quadratic terms can be used to describe the response and will be solely used in the following.

6 Estimates of damage intensity d

In this section, the bounds d^+ for the damage intensity are presented. These bounds, which have been defined in Eq. (10), are based on crossing intensities $\mu(u)$, which in turn, are computed using the algorithms presented in the appendices. The bounds are compared with the estimated damage intensities from simulated samples of the response $Y(t)$ and with the approximate bound, d^{poiss}, computed by means of Eq. (16).

Additionally, the method of transformed Gaussian process is used to approximate the response and compute the damage intensity in the process. The process is defined as follows.

Let $\tilde{Y}(t) = G(Y_L(t))$, where

$$G(u) = \begin{cases} \sqrt{-2\text{Var}(Y_L(0))\ln(\mu^a(u)/\mu^a(0))} \text{ if } u > 0, \\ -\sqrt{-2\text{Var}(Y_L(0))\ln(\mu^a(u)/\mu^a(0))} \text{ if } u < 0. \end{cases} \tag{43}$$

Here, $\mu^a(u)$ is the SORM approximation of the crossing intensity of the response process $Y(t)$, computed using the algorithm presented in Appendix 3.

The process $\tilde{Y}(t)$ crosses the level u with intensity $\mu^a(u)$. This is different from the crossing intensity of the response $\mu(u)$ for low u-levels. Since the two crossing intensities differ only for small u-levels, the difference is small (less than 5%) when checked by Monte Carlo simulations. This difference is smaller than discretization errors and are negligible in comparison with other sources of uncertainties.

This discrepancy in the computation of crossing intensities for low u-levels, is more than offset by the gain in the simplicity of the approach, which is a consequence of the fact that the zero upcrossing intensity of $Y_L(t)$ process is equal to $\mu^a(0)$, see Appendix 3. If it is required that $\tilde{Y}(t)$ to be transformed $Y_L(t)$ and has the mean level crossing rate equal to $\mu(u)$, then time also needs to be scaled, *i.e.*, $\tilde{Y}(t) = g(Y_L(c \cdot t))$ for some constant c.

The spectrum of $Y_L(t)$ is given in Fig. 3 while the transformation $G(\cdot)$ is shown in Fig. 11. However, before presenting the results, we make some comments on uncertainties while estimating the damage intensities.

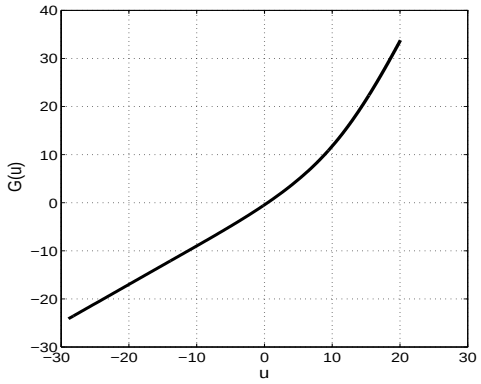

Fig. 11. The function $G(\cdot)$ for the transformed Gaussian approximation.

6.1 Uncertainties in estimation of damage intensity

When evaluating the quality of an approximation one is often comparing the computed damage intensity d for the damage functions $f(u,v) = (v-u)^b$, b taking values in a suitable interval. The damage intensity can be estimated from an observed (or simulated) load and can be compared against the derived approximation. We comment on three aspects of such comparisons.

Bias: As we have already discussed, due to the length T of the signal used to estimate the damage intensity, the observed damage is smaller (on an average) than the expected damage increment. This bias is due to the fact that the load is unknown before one starts to measure the signal, *i.e.*, $T_0 = 0$, while in the definition of d one assumes that the loads have been acting for a long time prior to measurements.

Variability of the damage: Obviously new measurements of the signal will give different estimates of the damage intensity d. In practice, one has only one estimate of d and hence, it is of interest to estimate how large is the statistical uncertainty, due to the finite length of observation interval T. Since we are comparing damage intensities d for different fatigue exponents b, it is more convenient to analyze the logarithms of the estimated damages. In Fig. 12, we present a normal probability plot for base 10 logarithms of the observed damage intensities (computed using Eq. 44), when $b = 6$ for two cases: (a) for time $T = 1500$ seconds (when the signal consist of about 500 cycles) and (b) $T = 3000$ seconds (which corresponds to a signal with about 1000 cycles), for an ensemble of 100 simulated signals of the response $Y(t)$. The dots to the right corresponds to the logarithms of damages for longer signals. We observe that the medians differ due to the bias ($T_0 = 0$) by 0.06, *i.e.*, 15% percent. Furthermore, the variance of the logarithms of d estimates slightly decreased from 0.2 to 0.18, for $b = 6$. We can therefore conclude that the statistical variability measured by standard deviation is much larger than the bias.

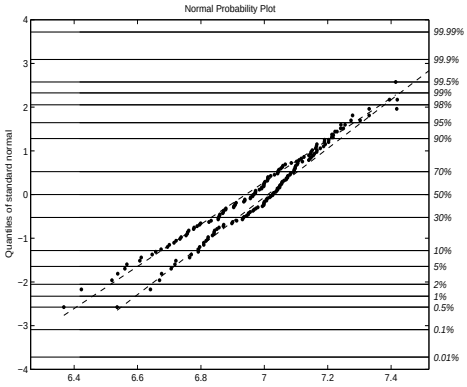

Fig. 12. Normal probability plot for base 10-logarithms of observed damage intensities.

Discretization errors: There are primarily two types of discretization errors. One possible source of discretization error is when one uses the following property of stationary and ergodic loads, viz. the damage intensity $d = \mathsf{E}[D_T]/T = \lim_{T\to\infty} D_T/T$, and hence

$$d \approx \frac{D_T}{T}. \tag{44}$$

However, often in field experiments, the real loads are saved in the form of a rain-flow matrix $p^{\mathrm{rfc}}(u, v)$. Subsequently, the damage intensity is computed using Eq. (5), viz.

$$d \approx \nu \int\int f(u, v) p^{\mathrm{rfc}}(u, v)\, \mathrm{d}u\, \mathrm{d}v \tag{45}$$

Computations of rain-flow matrices implies that the rain-flow cycles are discretized and this is the second source of discretization errors. Hence, the two approaches (Eqs. 44 and 45) may give different estimates for the damage intensity. There can be considerable differences for $f(u, v) = (v - u)^b$, when b is large. Consequently, if two methods have to be compared, one should use the same method for computing the damage, *i.e.*, by means of a direct sum or the rain-flow matrix.

6.1.1 Example of discretization error

We consider 100 simulated responses for $Y(t)$, each of duration 1500 s. For each signal, the damage was estimated using Eq.(44) and Eq.(45), with different values of damage exponent b. The logarithms of the damages are well approximated by the normal pdf with medians presented in Table 2. We see that the discretization error is about $10^{0.05} = 1.12$, *i.e.*, 10%, even if the rain-flow matrix contained 100 levels (which is more than what is common in practice).

Table 2
Median of $\log_{10}[d]$; differences due to discretization errors.

b	1	2	3	4	5	6
d (Eq. 44)	0.4476	1.5558	2.7903	4.1187	5.5272	6.9660
d (Eq. 45)	0.4785	1.5964	2.8367	4.1695	5.5755	7.0244

6.1.2 The transformed Gaussian approximation for the response

Here, we have simulated 100 samples of transformed Gaussian process $\tilde{Y}(t)$ of duration 1500 s. For each signal, the damage was estimated using Eq.(44) and Eq.(45), for different values of damage exponent b. The logarithms to the base 10, of the damages are very well approximated by the normal pdf with medians presented in Table 3. We see that the median damage for the transformed Gaussian process $\tilde{Y}(t)$ and that estimated from 100 simulations of the response $Y(t)$, are very close for $b \geq 3$ (the interesting levels), with the difference being less than 10%. For lower values of b, the approximation is less accurate due to underestimation of the crossings for low levels by the SORM-method.

Table 3
Median of the base 10 logarithms of the damage intensity for the transformed Gaussian approximation of the response, estimated using Eq. (44) and Eq. (45) with 100 signals of duration 1500 s.

b	1	2	3	4	5	6
d (Eq. 44)	0.4067	1.5061	2.7511	4.0966	5.5126	6.9717
d (Eq. 45)	0.4370	1.5429	2.7907	4.1375	5.5534	7.0202

The discretization errors are similar. However the loads are not equivalent from the fatigue point of view. In both cases, the estimates of the damage intensity are approximately log-normally distributed, with very similar median damage. However, the standard deviations of the logarithms are different. In Table 4, we give standard deviations of the base 10 logarithms of the estimated damages computed, for 100 realizations of $Y(t)$ of durations 1500 s.

It can thus be concluded that the large cycles are more evenly spread in the transformed Gaussian loads. In other words, on an average, there are as many large cycles in both models but the transformed Gaussian load has the numbers closer to the average.

6.2 Expected damage transformed Gaussian load

We turn now to the evaluation of the expected damage for the transformed Gaussian load. Note that the method approximates the sequence of the turning

Table 4
Standard deviations of the base 10 logarithms of the damage intensity for the transformed Gaussian approximation for the response, estimated using Eq. (44) and Eq. (45), for 100 signals of duration 1500 s.

b	1	2	3	4	5	6
$(\mathrm{Var}[d])^{0.5}$ (Eq. 44)	0.0253	0.0473	0.0730	0.1071	0.1503	0.2006
$(\mathrm{Var}[d])^{0.5}$ (Eq. 45)	0.0116	0.0207	0.0366	0.0614	0.0942	0.1331

points in $\tilde{Y}(t)$ by a Markov chain, with the Markov transition matrix computed from the spectrum $S(\omega)$ and the transformation $G(\cdot)$, see Fig. 3 and 11. Figure 13 illustrates the contour lines of the probabilities that the rain-flow cycles will have a maximum with height u_i and minimum with height u_j, with probability p_{ij}. Such a matrix could be called the expected rain-flow matrix normalized to have sum equal to unity. Figure 14 is the corresponding figure but defined for the min-max cycles. The contour lines are defined, such that, the probability of a point being outside the contour is known. Thus, if there are about 500 cycles in an observed time history, then it is expected that there would be about 5 cycles (represented by dots in Figs. 13-14) above the second contour, approximately 25 cycles above the third contour and so on. In Figs. 13 and 14, the rain-flow and Markov matrices are plotted along with the observed cycles. It can be seen that the rain-flow matrix is not too contradictory; only a few number of cycles with negative crests are overestimated in the transformed Gaussian load. The base 10 logarithms of the estimated damages, as b is varied from $1-6$ are respectively, 0.4312, 1.5487, 2.8084, 4.1647, 5.5896 and 7.0654. The values should be compared with the second row of Table 2. The bias analysis indicates that we could expect the values to be slightly higher, with a difference of about 0.08 for $b = 6$. The agreement is very good. We conclude that for the example studied in this paper, the transformed Gaussian approximation is sufficiently accurate.

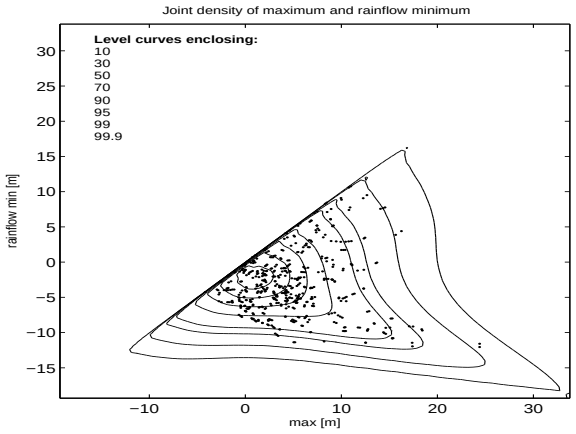

Fig. 13. Contours of normalized expected rain-flow matrix and observed rain-flow cycles.

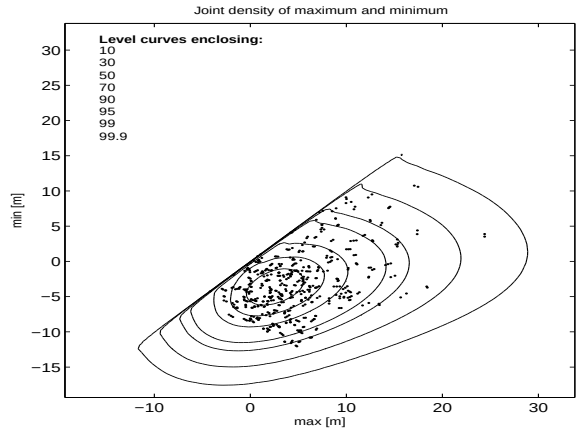

Fig. 14. Contours of normalized expected min-max matrix and observed min-max cycles.

6.3 The bounds and asymptotic Poisson correction

We next present the bounds, based on $\hat{\mu}(u,v)$ and $\tilde{\mu}(u,v)$, when the upcrossing intensities, $\mu(u)$, are computed using the algorithm in Appendix 1. The numerical estimates have been presented in Table 5. For $b=1$, the bound given in Table 5 is actually the exact fatigue damage and is not a bound. We observe that for higher values of b, the bounds are progressively higher. Thus, for $b=6$ the bound is about 60% higher than the damage estimated from 100 realizations of response $Y(t)$ of duration 1500 s. However, it must be noted that this overestimation has a 20% contribution from bias; see previous discussions. The Poisson corrected damage intensity is about 30% too high. This, though, is not very high, especially when compared to other uncertainties. On the other hand, the advantage of using the Poisson corrected approximation lies in its simplicity. Finally, in Table 6, we present the estimates of the damage intensity, where the up-crossing intensities, $\mu(u)$, are computed using the SORM approximation (Appendix 3). We observe that the approximations here are about 3% lower than the true bound and clearly could be used equivalently.

Table 5
Base 10-logarithms for the estimates for the upper bound and the Poisson corrected approximations for the expected rain-flow fatigue damage; mean crossing rates computed using algorithm presented in Appendix 1.

b	1	2	3	4	5	6
d^{+}	0.4520	1.6560	2.9524	4.3221	5.7518	7.2318
d^{poiss}	0.4520	1.6524	2.9396	4.2949	5.7081	7.1726

Table 6
Base 10-logarithms for the estimates for the upper bound and the Poisson corrected approximations for the expected rain-flow fatigue damage; mean crossing rates computed using SORM approximations

b	1	2	3	4	5	6
d^+	0.4169	1.6264	2.9278	4.3013	5.7337	7.2155
d^{poiss}	0.4169	1.6230	2.9154	4.2749	5.6911	7.1575

7 Concluding Remarks

A frequency domain based method has been developed for estimating the expected rain-flow fatigue damage in randomly vibrating structures, where the structure response is due to nonlinear combination of a vector of mutually correlated, stationary, Gaussian loads. The crux of the problem lies in estimating the mean up-crossing rate of the non-Gaussian structure response. For the special class of problems where the excitations can be modeled as quadratic functions of Gaussian loads, analytical approximations have been presented for the mean up-crossing rates for the structure response. Numerical algorithms have been developed which enable computing the level crossing statistics for problems not amenable for analytical solutions. Issues related to numerical efficiency and reduction in computational complexities have been addressed. Comparisons of the predictions using the proposed method have been carried out with available analytical techniques, such as SORM based asymptotic methods and with full scale Monte Carlo simulations. The proposed method leads to bounds for the expected rain-flow fatigue damage. A study has been carried out which investigates the quality of the bounds. A quantitative analysis has been carried out to identify sources of errors in the fatigue damage estimations. A comparative study of the predictions have been made when alternative approximations, such as, using transformed Gaussian loads and assuming Markov models for the loads. It can be concluded that the method proposed in this paper leads to fairly accurate estimates for the expected rain-flow fatigue damages. The required computational effort is significantly less than the existing time domain approaches and is commensurate with the analytical techniques available in the literature. Though the applicability of the proposed method has been demonstrated with respect to a wind vibration problem, the method can be used for studying the fatigue damage due to non-Gaussian load effects arising from other environmental loads also; see [18,22].

Acknowledgement

This work was supported in part by the Swedish Foundation for Strategic Research (SSF) via the Gothenburg Mathematical Modelling Center (GMMC).

References

[1] Baxevani A, Hagberg O, Rychlik I. Note on the distribution of extreme waves crests. Proc. 24th Int Conf Offshore Mech and Arctic Eng 2005.

[2] Benasciutti D, Tovo R. Cycle distribution and fatigue damage assessment in broad-band non-Gaussian random processes. Probab Eng Mech 2005;20(2):115-127.

[3] Bendat JS. Probability Functions for Random Responses: Prediction of Peaks, Fatigue damage and Catastrophic Failures. NASA technical report 1964.

[4] Benasciutti D, Tovo R. Spectral methods for lifetime prediction under wide band stationary random processes. Int J of Fatigue 2005;27:867-877.

[5] Bishop NWM, Sherratt. A theoretical solution for estimation of rainflow ranges from power spectral density data. Fatigue Frac Eng Mater Struct 1990;13:311-326.

[6] Bogsjo K. Stochastic modelling of road roughness. Licentiate of engineering thesis, Lund, Sweden; 2005.

[7] Breitung K. (1988) Asymptotic crossing rates for stationary Gaussian vector processes. Stoch Proc and Applications 1988;29:195-207.

[8] Brodtkorb PA, Johannesson P, Lingren G, Rychlik I, Rydén J, Sjö E. WAFO - a Matlab toolbox for analysis of random waves and loads. Proc of the 10th Int Offshore and Polar Eng Conf 2000;3:343-350.

[9] Ditlevsen O, Madsen HO. Structural reliability methods. Chichester: John Wiley and Sons; 1996.

[10] Frendahl M, Rychlik I. Rainflow analysis - Markov method. Int J of Fatigue 1993;15:265-272.

[11] Gupta S, Van Gelder P. Extreme value distributions for nonlinear transformations of vector Gaussian processes. Probab Eng Mech 2005; in press.

[12] Johannesson P. Rainflow Cycles for Switching Processes with Markov Structure. Probab in the Eng and Informational Sciences 1998;12(2):143-175.

[13] Johannesson P, Thomas JJ. Extrapolation of Rainflow Matrices. Extremes 2001;4:241-262.

[14] Krenk S, Gluver H. (1989) A Markov matrix for fatigue load simulation and rainflow range evaluation. Struct Saf 1989;6:247-258.

[15] Lindgren G. A note on the asymptotic independence of high level crossings for dependent Gaussian processes. Ann Probab 1974;2:535-539.

[16] Lindgren G. Extreme valus and crossings for the α-process and other functions of multidimensional Gaussian processes, with reliability applications. Adv Appl Probab 1980;12:746-774.

[17] Lindgren G, Broberg KB. Cycle range distributions for Gaussian processes - exact and approximate results. Extremes 2004;7:69-89.

[18] Machado UB. Statistical analysis of non-Gaussian environmental loads and responses. Ph.D. thesis, Lund Institute of Technology, Sweden; 2002.

[19] Matsuishi M, Endo T. Fatigue of metals subject to varying stress. Paper presented to Japan Soc Mech Engnrs, Jukvoka, Japan; 1968.

[20] Miner MA. Cumulative damage in fatigue. J Appl Mech 1945;12:A159-A164.

[21] Naess A. Prediction of extremes of stochastic processes in engineering applications with particular emphasis on analytical methods. Ph.D. Thesis, Trondheim, Norwegian Institute of Technology; 1985.

[22] Naess, A. Statistical analysis of nonlinear, second-order forces and motions of offshore structures in short-crested random seas. Probab Eng Mech 1990;5:110-118

[23] Palmgren, A. (1924) Die Lebensdauer von Kugellagern. *VDI Zeitschrift*, **68**, pp. 339-341.

[24] Petrucci G, Zuccarello B. Fatigue life prediction under wide band random loading. Fatigue Fract Engng Mater Struct 2004;27:1183-1195.

[25] Pitoiset X, Preumont A. Spectral methods for multiaxial random fatigue analysis of metallic structures. Int J of Fatigue 2000;22:541-550.

[26] Pitoiset X, Rychlik I, Preumont A. (2001) Spectral methods to estimate local multiaxial fatigue failure criteria for structures undergoing random vibrations. Fatigue Fract Engng Mater Struct 2001;24:715–727.

[27] Rice SO. A mathematical analysis of noise. In: Wax N, editor. Selected papers in random noise and stochastic processes. Dover Publications; 1956. p.133-294.

[28] Rychlik I. A new definition of the rainflow cycle counting method. Int J of Fatigue 1987;9:119-121.

[29] Rychlik I. Rain flow cycle distribution for ergodic load processes. SIAM J Appl Math 1988;48:662-679.

[30] Rychlik I. Rainflow cycles in Gaussian loads. Fatigue Fract Engng Mater and Struc 1992;15:57-72.

[31] Rychlik I. On the "narrow-band" approximation for expected fatigue damage. Probab Eng Mech 1993;8:1-4.

[32] Rychlik I. Note on cycle counts in irregular loads. Fatigue Fract Engng Mater Struc 1993;16:377-390.

[33] Rychlik I, Johannesson P, Leadbetter MR. Modelling and Statistical Analysis of Ocean-Wave Data using transformed Gaussian processes. Marine Structures 1997;10:13-47.

[34] Rychlik I, Gupta S. Rain-flow Fatigue Damage for transformed Gaussian Loads. Int J of Fatigue 2006; in press.

[35] Sobczyk K, Spencer BF. Random Fatigue: From Data to Theory. Academic Press, San Diego, 1992.

[36] Tovo R. Cycle distribution and fatigue damage under broad band random loading. Int J of Fatigue 2002;24:1137-1147.

[37] Wang X, Sun JQ. On the fatigue analysis of non-Gaussian stress processes with asymmetric distribution. J of Vibrations and Acoustics, ASME 2005;127:556-565

[38] Winterstein SR. Nonnormal responses and fatigue damage. J Eng Mech 1985;110:1291-1295.

[39] Winterstein SR. Nonlinear vibration models for extremes and fatigue. J Eng Mech 1988;114:1772-1790.

[40] Wirshing PH, Light MC. Fatigue under wide band random loading. J Struct Div ASCE 1980;106(7):1593-1607.

A Appendix 1

We first rewrite the joint pdf $p_{Y\dot{Y}}(\cdot,\cdot)$ in the form

$$p_{Y\dot{Y}}(y,\dot{y}) = \int_{-\infty}^{\infty} ... \int_{-\infty}^{\infty} p_{X_2...X_nY\dot{Y}}(x_2,..,x_n,y,\dot{y})\mathrm{d}x_2..\mathrm{d}x_n, \tag{A.1}$$

where, $p_{X_2...X_nY\dot{Y}}(\cdot)$ is the joint pdf of random variables X_2,...,X_n, Y and $\dot{Y}$, at time t. We seek the transformation between the joint pdf $p_{X_2..X_nY\dot{Y}}(\cdot)$ and $p_{X_1..X_n\dot{Y}}(\cdot)$. We assume that at time t, Y in Eq. (1), is a function of X_1 with all the other random variables being fixed. Thus, from Eq. (1), given by

$Y = g(X_1, x_2, ..., x_n)$, we assume that there are k solutions for X_1 for a given set of values $Y = y, X_2 = x_2, .., X_n = x_n$. This leads to the expression

$$p_{X_2..X_nY\dot{Y}}(x_2, ..., x_n, y, \dot{y}) = \sum_{i=1}^{k} \left| \frac{\partial Y}{\partial X_1} \right|_i^{-1} p_{X_1X_2..X_n\dot{Y}}(x_1, x_2, ..., x_n, \dot{y}), \quad \text{(A.2)}$$

$y = g(x_1, x_2, ..., x_n)$. The joint pdf $p_{X_1...X_n\dot{Y}}(\cdot)$ is now written as

$$p_{X_1..X_n\dot{Y}}(x_1, .., x_n, \dot{y}) = p_{\dot{Y}|X_1..X_n}(\dot{y}|X_1 = x_1, .., X_n = x_n)\Pi_{j=1}^{n} p_{X_j}(x_j), \quad \text{(A.3)}$$

since $\mathbf{X}$ is assumed to be a vector of mutually independent Gaussian random variables, $p_{X_1..X_n}(x_1, .., x_n) = \Pi_{j=1}^{n} p_{X_j}(x_j)$.

$\dot{Y}(t)$ is obtained by differentiating Eq. (1) with respect to t, and when conditioned on $\{X_j = x_j\}_{j=1}^{n}$, is given by

$$\dot{Y}|_{\mathbf{X}} = \sum_{i=1}^{n} \left| \frac{\partial Y}{\partial X_i} \right|_{\mathbf{X}} \dot{X}_i = \sum_{i=1}^{n} g_i \dot{X}_i = \mathbf{G}\dot{\mathbf{X}}. \quad \text{(A.4)}$$

Here, the vector $\mathbf{G} = [g_1, .., g_n]$, $\dot{\mathbf{X}} = [\dot{X}_1, .., \dot{X}_n]'$, the superscript $(')$ denoting transpose, $g_i = \partial Y/\partial X_i$ and when conditioned on $\mathbf{X}$, is a constant. $\dot{X}(t)$ are the time derivatives of $X(t)$ and are also zero-mean stationary, Gaussian random processes. Thus, $\dot{Y}|_{\mathbf{X}}$ in Eq. (A.4) is a linear sum of Gaussian random variables and is a Gaussian random variable with parameters

$$\begin{aligned}
\mu_{\dot{Y}|\mathbf{X}} &= \mathsf{E}[\dot{Y}|\mathbf{X} = \mathbf{x}] = \mathbf{G}\{\mathsf{E}[\dot{\mathbf{Y}}] + \mathrm{Cov}(\dot{\mathbf{X}}, \mathbf{X})\mathrm{Cov}(\mathbf{X}, \mathbf{X})^{-1}(\mathbf{x} - \mathsf{E}[\mathbf{X}])\} \\
&= \mathbf{G}\mathrm{Cov}(\dot{\mathbf{X}}, \mathbf{X})\mathbf{x}, \\
\sigma^2_{\dot{Y}|\mathbf{x}} &= \mathrm{Var}[\dot{Y}|\mathbf{X} = \mathbf{x}] = \mathbf{G}\{\mathrm{Var}[\dot{\mathbf{X}}] - \mathrm{Cov}(\dot{\mathbf{X}}, \mathbf{X})\mathrm{Cov}(\mathbf{X}, \mathbf{X})^{-1}\mathrm{Cov}(\mathbf{X}, \dot{\mathbf{X}})\} \\
&= \mathbf{G}[\mathbf{C}_{\dot{\mathbf{X}}\dot{\mathbf{X}}} - \mathbf{C}'_{\mathbf{X}\dot{\mathbf{X}}}\mathbf{C}_{\mathbf{X}\dot{\mathbf{X}}}]\mathbf{G}'. \quad \text{(A.5)}
\end{aligned}$$

Here, $\mathsf{E}[\cdot]$, $\mathrm{Var}[\cdot]$ and $\mathrm{Cov}[\cdot]$ respectively denote the mean, variance and the covariance.

Substituting Eqs. (A.1-A.5) in Eq. (11), the mean up-crossing rate is given by

$$\mu_Y(u) = \sum_{i=1}^{k} \int\limits_{\Omega_i}^{\cdot\cdot} \int |h_1^{(i)}|^{-1} \Big\{ \int_0^\infty \dot{y} p_{\dot{Y}|\mathbf{X}}(\dot{y}; \mathbf{x}^{(i)}) \mathrm{d}\dot{y} \Big\} p_{X_1}(x_1^{(i)}) \prod_{j=2}^{n} p_{X_j}(x_j) \mathrm{d}x_2..\mathrm{d}x_n. \quad \text{(A.6)}$$

Here, $\mathbf{x}^{(i)} = [x_1^{(i)}, x_2, .., x_n]$, $h_1^{(i)} = \left| \frac{\partial Y}{\partial X_1} \right|_{\mathbf{X}^{(i)}}$, and Ω_i denotes the domain of integration determined by the permissible set of values $x_2, ..., x_n$ for each solution of $x_1^{(j)}$. Since $p_{\dot{Y}|\mathbf{X}}(\cdot)$ is Gaussian, it can be shown that [21]

$$\int_0^\infty \dot{v} p_{\dot{Y}|\mathbf{X}}(\dot{y}; \mathbf{x}) \mathrm{d}\dot{y} = \sigma_{\dot{Y}|\mathbf{X}} \Psi\Big(\frac{\mu_{Y|\mathbf{X}}}{\sigma_{Y|\mathbf{X}}} \Big), \quad \text{(A.7)}$$

where, $\Psi(x) = \phi(x) + x\Phi(x)$ and $\phi(x)$ and $\Phi(x)$ are respectively the standard Gaussian pdf and the standard Gaussian probability distribution function (PDF). Thus, Eq. (A.6) can be expressed as

$$\mu_Y(u) = \sum_{i=1}^{k} \int_{\Omega_i}^{\cdots} \int \tilde{f}(x_1^{(i)}, x_2, .., x_n) \prod_{j=2}^{n} p_{X_j}(x_j) \mathrm{d}x_j, \tag{A.8}$$

where, $\tilde{f}(x_1^{(i)}, x_2, .., x_n) = |h_1^{(i)}|^{-1} \sigma_{\dot{Y}|\mathbf{X}} \Psi\left(\frac{\mu_{\dot{Y}|\mathbf{X}}}{\sigma_{\dot{Y}|\mathbf{X}}}\right) p_{X_1}(x_1^{(i)})$. This approach had been first proposed in [21] and closed form expressions for a limited class of problems had been presented.

The scope of this approach had been extended in [11] to a wider class of problems. The difficulties involved in evaluating $\mu_Y(u)$ from Eq. (A.8) are (a) determining the domain of integration Ω_i, defined by the possible set of solutions for $X_1^{(i)}$, and (b) evaluation of the multidimensional integrals

$$I_j = \int_{\Omega_j}^{\cdots} \int \tilde{f}(x_1^{(j)}, x_2, .., x_n) \prod_{j=1}^{n} p_{X_j}(x_j) \mathrm{d}x_j, \tag{A.9}$$

where the dimension of the integral, I_j is $(n-1)$. Questions addressing the solution of these integrals using the Monte Carlo method has been discussed in [11]. In this paper, we employ the Monte Carlo integration method for computing $\mu_Y(u)$.

B Appendix 2

For structure responses written as

$$Y(t) = \sum_{j=1}^{k+1} \{\Gamma_j X_j(t) + \frac{\Lambda_j}{2} X_j^2(t)\} \tag{B.1}$$

where, $\Lambda_{k+1} = 0$, one can express $Y(t)$ as a combination of a Gaussian and a non-Gaussian process, in the form

$$Y(t) = \sum_{j=1}^{k} \{\Gamma_j X_j(t) + \frac{\Lambda_j}{2} X_j^2(t)\} + \Gamma_{k+1} X_{k+1}(t) = Y_{NG}(t) + Y_G(t). \tag{B.2}$$

We rewrite $p_{Y\dot{Y}}(y, \dot{y})$ in terms of a joint pdf of the random variables $X_1, .., X_k$ and get

$$p_{Y\dot{Y}} = \int_{-\infty}^{\infty} ... \int_{-\infty}^{\infty} p_{X_1 X_2 .. X_k Y \dot{Y}}(x_1, .., x_k, y, \dot{y}) \mathrm{d}x_1 .. \mathrm{d}x_k. \tag{B.3}$$

Subsequently, we follow an identical procedure as detailed in Appendix 1. However, the difference is that now the first k random variables are used

rather than the last k in the vector $\mathbf{X}$. This is advantageous for quadratic forms as for given values of $Y = y$, $X_1 = x_1, .., X_k = x_k$, there exists only one solution for X_{k+1}, given by

$$x_{k+1} = y - \sum_{j=1}^{k} \{\Gamma_j x_j + \frac{\Lambda_j}{2} x_j^2\}. \tag{B.4}$$

Also, the domain of integration for the multi-dimensional integrals is $[-\infty, \infty]$. This leads to the simpler form for $\mu_Y(y)$, given by

$$\begin{aligned} \mu_Y(y) &= \int_{-\infty}^{\infty} .. \int_{-\infty}^{\infty} \frac{1}{J} \{\sigma_{\dot{Y}|\mathbf{X}} \Psi\Big(\frac{\mu_{\dot{Y}|\mathbf{X}}}{\sigma_{\dot{Y}|\mathbf{X}}}\Big) p_{X_{k+1}}(x_{k+1})\} \prod_{j=1}^{k} p_{X_j}(x_j) \mathrm{d}x_j \\ &= \frac{1}{\Gamma_{k+1}} \mathsf{E}[\sigma_{\dot{Y}|\mathbf{X}} \Psi\Big(\frac{\mu_{\dot{Y}|\mathbf{X}}}{\sigma_{\dot{Y}|\mathbf{X}}}\Big) p_{X_{k+1}}(x_{k+1})]_{X_1 \dots X_k}, \end{aligned} \tag{B.5}$$

where, $J = \mathrm{d}Y/\mathrm{d}X_{k+1} = \Gamma_{k+1}$ and x_{k+1} depends on $X_1, ..X_k$. The parameters $\sigma_{\dot{Y}|\mathbf{X}}$ and $\mu_{\dot{Y}|\mathbf{X}}$ are computed as in Appendix 1.

C Appendix 3

The following generalization of Breitung's approximation [7] can be found in [1]. The formulae presented here are, in principle, explicit, although they require finding the design point. In comparison with the Monte Carlo (MC) simulation approach, presented in Appendices 1 and 2, the disadvantage in this method is that for small levels u the formulaes are only approximations. On the other hand, for higher (and often more important) levels u, the formulaes are very accurate, but requires the identification of the design point. Note that the MC-methods can not be used to compute crossings of very high levels, e.g. $\mu(u) < 10^{-6}$. In such a case importance sampling has to be used and that would in turn, require identification of the design points. In that case, the MC method would give similar result to the asymptotic approach however with much higher computational effort.

Theorem 1 *Let $g : \mathbb{R}^n \to \mathbb{R}$ be a function such that the surface*

$$S = \{\mathbf{x} = (x_1, \dots, x_n); g(\mathbf{x}) = 0\}$$

has a point $\mathbf{x}_0$ such that $||\mathbf{x}_0|| = 1$ and $||\mathbf{x}|| > 1$ for all other $\mathbf{x} \in S$. By $\mathbf{x}$ we denote both the vector $(x_1, \dots, x_n)$ and the $n \times 1$ column matrix. Suppose $\mathbf{Z}(t)$ is an n-dimensional, stationary, differentiable, Gaussian vector process, and let $\dot{\mathbf{Z}}(t)$ denote its derivative. The correlation of the vector $(\mathbf{Z}(t), \dot{\mathbf{Z}}(t))$ is

denoted by Σ,

$$\Sigma = \begin{bmatrix} I & \Sigma_{12} \\ \Sigma_{21} & \Sigma_{22} \end{bmatrix}. \tag{C.1}$$

For a family of processes $g(\mathbf{Z}(t)/\beta)$, $\beta > 0$, *under some mild technical assumptions, the intensity of zero up-crossings is given by*

$$\mu_\beta(0) = \frac{e^{-\beta^2/2}}{2\pi}(c + O(\beta^{-2})), \qquad c = \sqrt{\frac{\mathbf{x}_0^T \left(\Sigma_{22} - \Sigma_{21} G_0 \Sigma_{12}\right) \mathbf{x}_0}{\det\left(I + P_0 G_0 P_0\right)}}, \tag{C.2}$$

as β *tends to infinity, where* $G_0 := \frac{1}{|\nabla g(\mathbf{x}_0)|}\left[\frac{\partial^2 g}{\partial x_i \partial x_j}(\mathbf{x}_0)\right]_{i,j=1,2,\ldots,n}$ *and* $P_0 := I - \mathbf{x}_0\mathbf{x}_0^T$.

Since $\mathbf{Z}(t)$ *is stationary, the same formula is valid for down-crossings.*

Based on the above theorem, the following remarks can be made:

(1) Formula (C.2) is in a sense finitely additive, *i.e.*, if there are a finite number of points with minimal distance to the origin, the asymptotic formula for the upcrossing intensity of the process $g(\mathbf{Z}(t)/\beta)$ is the sum of the upcrossing intensities estimated using Eq. (C.2) for each point separately. Breitung's asymptotic approximation fails in the case of an infinite number of such points.
(2) Theorem 1 is a generalization of Breitung's result in two sense: In contrast to Theorem 1, Breitung demands the surface S to be finite, and Theorem 1 contains the order of the error term.
(3) Theorem 1 lends itself to a geometric interpretation. Note that $g(\mathbf{Z}(t)/\beta)$ crosses the zero level, if and only if, the vector process $\mathbf{Z}(t)$ crosses the surface βS. Hence, instead of saying that the formula is asymptotic "as β tends to infinity" we may say "as the surface S is inflated".
(4) The simpler FORM approximation is derived by assuming that locally at the design point $\mathbf{x}_0$ the curvature of the surface is zero, *i.e.*, G_0 is a matrix containing only zeros giving the following approximation

$$\mu_\beta(0) \approx \frac{\mathrm{e}^{-\beta^2/2}}{2\pi}\sqrt{\mathbf{x}_0^T \Sigma_{22} \mathbf{x}_0}. \tag{C.3}$$

Here, we are interested in quadratic processes of type

$$Y(t) = \sum_{j=0}^{n} \gamma_j X_j(t) + \sum_{j=0}^{n} \frac{\lambda_j}{2} X_j(t)^2, \tag{C.4}$$

where $\mathbf{X}(t) = (X_0(t), \ldots, X_n(t))$ is a vector of stationary Gaussian process, such that, for each t, $X_j(t) \in N(0,1)$ and the variables $X_j(t) \perp X_k(t)$. Denote $\dot{\mathbf{X}}(t) = (\dot{X}_0(t), \ldots, \dot{X}_n(t))$. Let the correlation structure of $\mathbf{X}(t), \dot{\mathbf{X}}(t)$ be given

by Eq. (C.1). We shall now demonstrate how the theorem can be used to approximate $\mu(u)$, the upcrossing intensity of the level u by the process $Y(t)$ defined in Eq. (C.4).

Gaussian case, all $\lambda_i = 0$

Let us consider two special cases when the stress is a Gaussian process *i.e.*, the quadratic correction term in Eq. (C.4) may be ignored. This implies that $\lambda_j = 0$. Thus, Eq. (C.4) simplifies to $Y(t) = \gamma^{'}\mathbf{X}(t)$, where $\gamma = (\gamma_1, \ldots, \gamma_{2N})$. Define

$$g(\mathbf{x}) = 1 - \frac{1}{||\gamma||}\gamma^{'}\mathbf{x}, \tag{C.5}$$

and note that, if $\beta = u/||\gamma|| := \beta_u$, the process $g(\mathbf{X}(t)/\beta)$ down-crosses the zero level exactly when $Y(t)$ up-crosses the level u. (Here $||\cdot||$ denotes norm in R^n, *e.g.*, $||\gamma||^2 = \sum \gamma_j^2 = \mathrm{Var}[X(0)]$.) On the surface $g(\mathbf{x}) = 0$, the point closest to the origin is $\mathbf{x}_0 = \gamma/||\gamma||$, and since all second order derivatives of g are zero, Breitung's approximation gives

$$\mu_\beta(0) = \frac{1}{2\pi}\frac{\sqrt{\gamma^{'}\Sigma_{22}\gamma}}{||\gamma||}\exp\left(\frac{-\beta_u^2}{2}\right), \tag{C.6}$$

since $\mathbf{x}_0 = \gamma/||\gamma||$. As expected the approximation is exact, as given by Rice's formula for a Gaussian process, since with $\mathrm{Var}[X(0)] = ||\gamma||^2$ and $\mathrm{Var}[\dot{X}(0)] = \gamma\Sigma_{22}\gamma^{'}$.

Pure quadratic case, all $\gamma_i = 0$

Suppose next that the linear term in Eq. (C.4) is negligible. In this case, we may write $Y(t) = \frac{1}{2}\mathbf{X}(t)^{'}\Lambda\mathbf{X}(t)$, where $\Lambda = \mathrm{diag}\left([\lambda_1, \ldots, \lambda_n]\right)$ is the diagonal matrix, with $\prod_{i=1}^n \lambda_i \neq 0$. We also assume that $\lambda_1 \leq \lambda_2 \leq \cdots \leq \lambda_n$. Additionally, for $u > 0$, we need to assume that $\lambda_n > 0$, since otherwise $Y(t) \leq 0$ for all t. By defining

$$g(\mathbf{x}) = 1 - \frac{1}{\lambda_n}\mathbf{x}^{'}\Lambda\mathbf{x}, \tag{C.7}$$

it can be seen that for $\beta = \sqrt{2u/\lambda_n} := \beta_u$, the zero down-crossing intensity of the process $g(\mathbf{X}(t)/\beta)$ equals the upcrossing intensity of the level u by the process $Y(t)$. Consequently, $\mu_\beta(0) = \mu(u)$ and Theorem (1) may be used to compute $\mu_\beta(0)$. Note, however, that there are two points

$$\mathbf{x}_\pm := \pm\begin{bmatrix} 0 & 0 & \ldots & 1 \end{bmatrix}^{'} \tag{C.8}$$

of minimal distance to the origin. Hence, one has to compute formula (C.2) for each one of these points separately ($G_0 = -\frac{1}{\lambda_n}\Lambda$ for both points), and add

the results. Consequently, by Theorem 1,

$$\mu(u) = \frac{1}{\pi}\exp(-\frac{h}{\lambda_n})\left(\sqrt{\frac{\mathrm{Var}[\dot{X}_n(0)] - \sum_{i=1}^{n}(\lambda_i/\lambda_n)\mathrm{Cov}(X_i(0),\dot{X}_n(0))^2}{(1-\lambda_1/\lambda_n)\ldots(1-\lambda_{n-1}/\lambda_n)}} + O(h^{-1})\right), \tag{C.9}$$

since we have two design points.

Note that $\mu(v)$ for $v < 0$ one can use the Eq. (C.9) with $u = -v$ and by changing signs of λ_i, which has to be again ordered into increasing order.

General quadratic loads:

Before proceeding further, it should be emphasized that Theorem 1 for the two cases of purely linear/quadratic loads gave asymptotic formulas *as the level tends to infinity*. The general case is more complicated. This is not surprising since we have the mix of two different limiting cases. We have to construct somewhat artificial asymptotics. The idea is as follows. Fix the level u, assumed to be large, and let

$$p(\mathbf{x}) := \gamma'\mathbf{x} + \frac{1}{2}\mathbf{x}^T\Lambda\mathbf{x}. \tag{C.10}$$

Assume that there is only one point $\mathbf{x}_u$ on the surface

$$\{\mathbf{x} \in \mathbb{R}^n; p(\mathbf{x}) = u\} \tag{C.11}$$

of minimal distance to the origin, and define $\beta_u := ||\mathbf{x}_u||$. Let

$$g(\mathbf{x}) := 1 - \frac{1}{u}\left(\beta_u\gamma'\mathbf{x} + \beta_u^2\frac{1}{2}\mathbf{x}'\Lambda\mathbf{x}\right). \tag{C.12}$$

As before, the process $g(\mathbf{X}(t)/\beta_u)$ crosses the zero level when the process $p(\mathbf{X}(t))$ crosses the level u; hence, using Breitung's method, with $\mathbf{x}_0 = \mathbf{x}_u/\beta_u$, for each level u separately, we have $\mu_{\beta_u}(0)$ equal to the u-upcrossing intensity for the process $p(\mathbf{Z}(t))$. Therefore, it is reasonable to believe that if β_u is large, then the term $O(\beta^{-2})$ for $\beta = \beta_u$ is small. Hence the approximation is good. However, the problem is that for each value u one has to find the design point $\mathbf{x}_u$ and define a new function $g(\cdot)$. This implies that we cannot use the theorem, which is valid for a fixed g, to motivate that the error term decreases to zero as h tends to infinity.

However, there are good reasons to use Breitung's approximation in this way instead of a formula which is truly asymptotic as the level u tends to infinity, especially if the linear terms dominate over the quadratic for the levels of interest, u. This is because, for u large enough, the u-crossings of the process will almost exclusively depend on the quadratic part. In contrast for u-level

close to zero ($\beta_u \approx 0$) the quadratic term in Eq. (C.10) is negligible and one has the pure Gaussian case. Note that the method approximates the zero crossing intensity by zero crossing intensity in the pure Gaussian process. It is suggested that the use of Breitung's method will give a proper balance between the linear and the quadratic terms.

We turn now to the computation of Breitung's approximation

$$\mu_{\beta_u}(0) = \exp(-\beta_u^2/2)c(\beta_u)/2\pi, \tag{C.13}$$

given in Theorem 1. Note that, opposed to the formulation in Theorem 1, we indicate c's dependence of β_u. Evaluating the terms gives

$$\begin{aligned} \nabla g(\mathbf{x})^{'}|_{\mathbf{x}=\mathbf{x}_u/\beta_u} &= -\left(\frac{\beta_u}{u}\gamma + \frac{\beta_u^2}{u}\Lambda\mathbf{x}\right)|_{\mathbf{x}=\mathbf{x}_u/\beta_u} = -\frac{\beta_u}{u}\left(\gamma + \Lambda\mathbf{x}_u\right), \\ G_0 &= \frac{-\beta_u\Lambda}{||\left(\gamma + \Lambda\mathbf{x}_u\right)||}\Lambda \quad P_0 = I - \frac{1}{\beta_u^2}\mathbf{x}_u\mathbf{x}_u^{'}. \end{aligned} \tag{C.14}$$

Now we can use the following approximation

$$\mu(u) \approx \frac{\mathrm{e}^{-\beta_u^2/2}}{2\pi}c(\beta_u), \tag{C.15}$$

where

$$c(\beta_u) = \sqrt{\frac{\mathbf{x}_u^T\left(\Sigma_{22} - \Sigma_{21}G_0\Sigma_{21}\right)\mathbf{x}_u}{\beta_u^2\det\left(I + P_0G_0P_0\right)}} \tag{C.16}$$

The simpler FORM approximation is, by Eq.(C.3), given by

$$\mu(u) \approx \mathrm{e}^{-\beta_u^2/2}\frac{\sqrt{\mathbf{x}_u^T\Sigma_{22}\mathbf{x}_u}}{2\pi\beta_u}. \tag{C.17}$$

It must be noted that the point of minimum norm, $\mathbf{x}_u$, can be found by standard optimization methods, see [9].